0.4 μm spatial resolution with 1 GHz ($\lambda = 30$ cm) evanescent microwave probe

M. Tabib-Azar,[a] D.-P. Su, and A. Pohar
Electrical Engineering and Applied Physics, Case Western Reserve University, Cleveland, Ohio 44106-7221

S. R. LeClair
Air Force Research Laboratory, Materials & Manufacturing Directorate, Wright–Patterson Air Force Base, Ohio

G. Ponchak
NASA Lewis Research Center, Cleveland, Ohio

(Received 16 October 1998; accepted for publication 2 December 1998)

In this article we describe evanescent field imaging of material nonuniformities with a record resolution of 0.4 μm at 1 GHz ($\lambda_g/750\,000$), using a resonant stripline scanning microwave probe. A chemically etched tip is used as a point-like evanescent field emitter and a probe–sample distance modulation is employed to improve the signal-to-noise ratio. Images obtained by evanescent microwave probe, by optical microscope, and by scanning tunneling microscope are presented for comparison. Probe was calibrated to perform quantitative conductivity measurements. The principal factors affecting the ultimate resolution of evanescent microwave probe are also discussed. © *1999 American Institute of Physics.* [S0034-6748(99)03603-5]

I. INTRODUCTION

There is a growing demand to develop nondestructive and noncontact imaging techniques with very high resolution. For example, mapping defects and variations in carrier concentration with submicron resolution is very desirable for the semiconductor industries as the devices are scaled down. Imaging the complex conductivity change in biological samples reveals the variations of physiological state and can be used for diagnostic purpose. The studies of novel high T_c superconductors and magnetoresistive materials are some of the other potential applications. The ability of obtaining the microwave resistivity information is the unique feature of microwave microscopy. Another advantage of microwave probing is its larger penetration depth, which makes the subsurface properties of the sample detectable as well as the surface properties.

To get micron/submicron resolution using microwaves, evanescent electromagnetic fields must be used to surpass the well-known Abbe barrier, which sets the classical limit of minimum resolvable size as 1/2 of the wavelength λ (on the order of centimeters for microwave) of the excitation fields. In nature, the Abbe barrier is a spatial version of ''sampling theorem'': to fully recover a signal, one has to recover all the spatial frequency components of it. In near field, however, the evanescent waves decay exponentially in space, therefore they contain frequencies higher than $1/\lambda$. The fact that evanescent waves are more confined than the single tone sinusoid waves and hence contain wider range of spatial frequencies indicates that it may be possible to have no theoretical limit of resolution for near field probes. The practical limit is set by the instrument sensitivity and the probe (tip) geometry that dictates the decay rate.

Evanescent microwave fields were first used by Ash and Nicholls[1] in a test rig to demonstrate their imaging ability. They achieve a resolution of $\lambda/60$ in one dimension and $\lambda/20$ in two dimensions, using a microwave radiation with $\lambda = 3$ cm. Tabib-Azar, Shoemaker, and Harris[2] used a microstripline quarter-wavelength resonator and extended Ash's work to semiconductor characterization with a resolution of $\lambda/1000$ in early 1990s.[3] Steinhauer used a 2 m long resonant coaxial transmission line as the key element and achieved 100 μm resolution in 1997 (20 μm resolution was reported later by this group with their probe operated at 10 GHz). Recently, Gao and co-workers[4] were credited with a record resolution of 0.1 μm at 3 GHz. They used essentially a three-dimensional (3D) rectangular waveguide structure and kept the tip in contact with the sample during scanning.

We hereby report a novel evanescent microwave probe (EMP) with a 0.5 μm resolution at 1 GHz ($\lambda/750\,000$). Images generated by EMP, optical microscope, and scanning tunneling microscope (STM) are presented for comparison. Several advantages of our probe in addition to its high spatial resolution are: there is no contact between the tip and the sample during scanning, and therefore, absolutely nondestructive and noncontact. Moreover, we use two-dimensional (2D) stripline structure as the resonator, which can be integrated with on-board electronics on silicon. Furthermore, the EMP is calibrated to perform quantitative measurements of conductivity.

II. EXPERIMENTAL PROCEDURES

The key element of EMP is a stripline resonator (see Fig. 1). One end of the stripline is connected to a tapered stainless steel wire as the probe tip, and the other end is coupled by a three-fingered interdigitated capacitor to a short feed line.

[a]Electronic mail: mxt7@po.cwru.edu

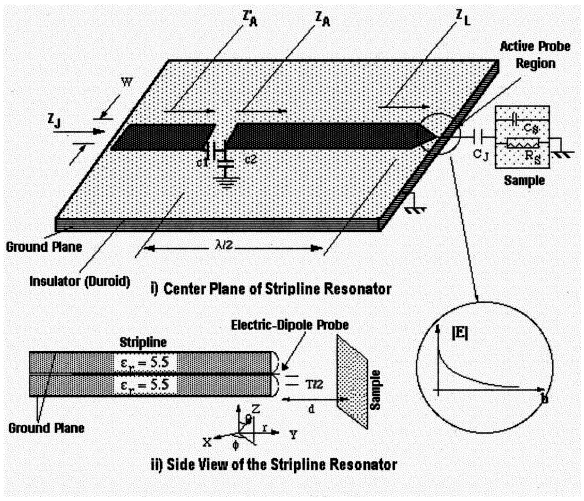

FIG. 1. Stripline resonator and probe assembly.

The feed line is connected to a three-port circulator, which circulates the signal from the radio frequency source to the resonator, and directs the reflected wave to a crystal detector. The sample is mounted on an X-Y stage and scanned underneath the probe tip (see Fig. 2). We operated the probe at a fixed frequency (around 1 GHz) and measured the crystal detector's output. This way we could generate 2D images of various planar samples.

We modeled[5] the stripline resonator (open circuit transmission line) by a series LCR circuit [shown in Fig. 3(a)] near its resonance frequency. When a sample is placed near the tip, its electromagnetic properties are coupled to the LCR circuit through a coupling capacitor. For simplicity, conductors and insulators are modeled in Figs. 3(b) and 3(c), respectively. In these figures, R_0, L_0, and C_0 are the intrinsic circuit parameters of the stripline resonator; C_c models the coupling capacitance of the air gap between the tip and sample; L_s, C_s, and R_s model the microwave properties of the sample. The resonance frequency shifts in the presence of a sample near the probe tip.

From these circuit models, it is clear that the shift in resonance frequency (and therefore the probe data output) depends on both the complex conductivity of the sample and on the probe–sample distance. To quantitatively map the surface conductivity, we placed a reflectance-compensated fiber optic distance sensor right next the tip of the probe, and

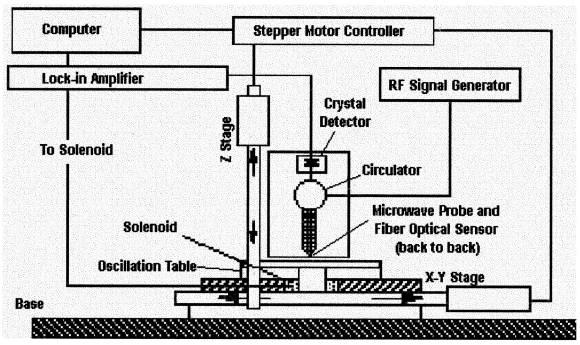

FIG. 2. EMP device experimental setup diagram.

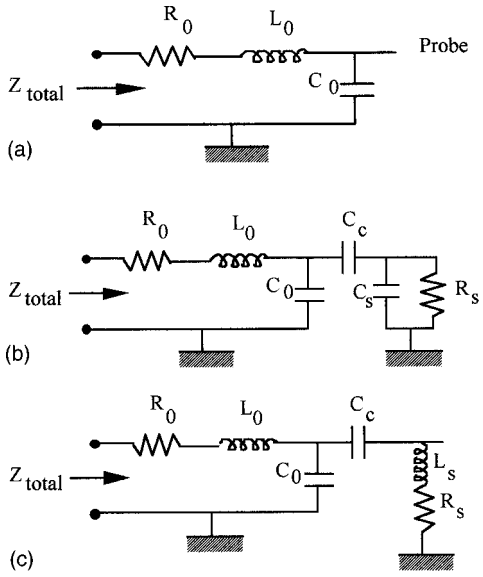

FIG. 3. (a) Series of lumped LCR models of the evanescent microwave probe. (b) Circuit model in presence of an insulating sample. (c) Circuit model in presence of a conducting sample.

performed a distance feedback control (in Z direction) to alleviate dependence of the probe output on the topography of the sample surface. Currently, the accuracy of distance control is around 0.4 μm.

To improve the resolution of the EMP, two nonexclusive methods can be used. One is to increase the signal-to-noise (S/N) ratio of the system; the other is to confine the field pattern. In the first approach, we performed synchronized measurement: By vibrating the sample with a 100 Hz oscillation, the modulated signal was fed to a lock-in amplifier for synchronous detection. With fine adjustment, the unevenness of oscillation could be made less than 0.5% across a sample of 1 in. diam. Figure 4 shows the line scans of a 125 μm wire using both synchronized and asynchronized methods. The improvement effect of S/N is obvious, and it results in sharper linewidths. Another reason for improved resolution is an effective reduction in the sample-to-probe distance due to the vibration of the sample.

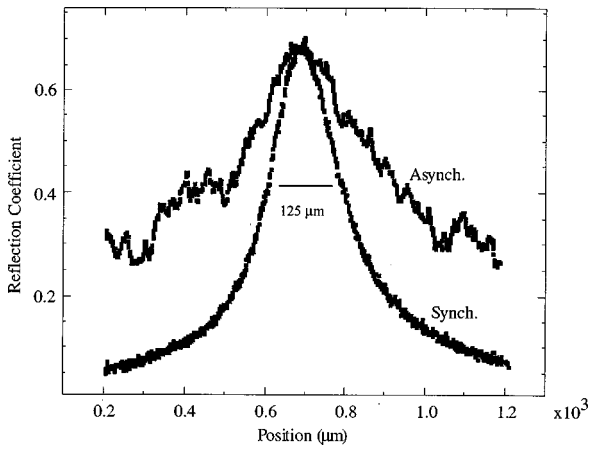

FIG. 4. EMP scan of a metallic wire of 125 μm diam. The synchronized measurement results in a much better resolution than asynchronized measurement.

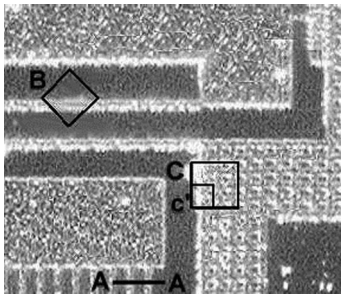

FIG. 5. Optical image of the structure from a MEMS chip that is scanned with EMP and STM instruments.

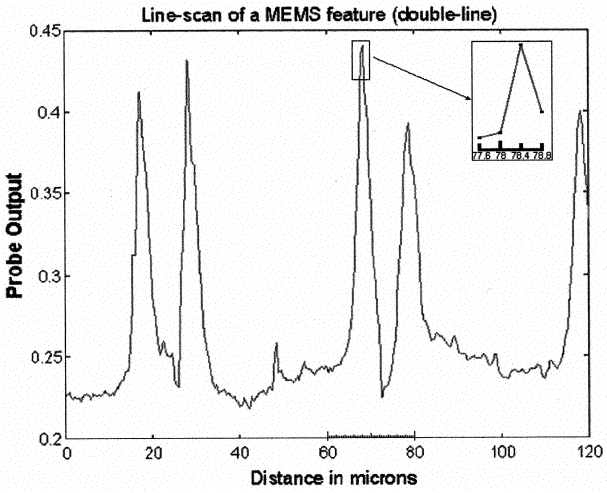

FIG. 6. 1D EMP scan of a double line feature (*A*-*A* shown in Fig. 5).

III. EXPERIMENTAL RESULTS

The second approach is to confine the field patterns. We used a chemically etched stainless steel wire as the tip. The original wire was 20 μm in diameter. After tapering, we observed the tip geometry using an optical microscopy and estimated the effective tip size as 1–2 μm. In addition, we reduced the size of the aperture of the probe opening to about 1 mm^2, which reduced the background noise and contributed to a higher Q value of the resonator. We also changed the configuration of the resonator from microstripline to stripline to reduce radiation losses and improve the resonator's Q.

To test the spatial resolution of the EMP system, we chose a microelectromechanic structure (MEMS) chip for

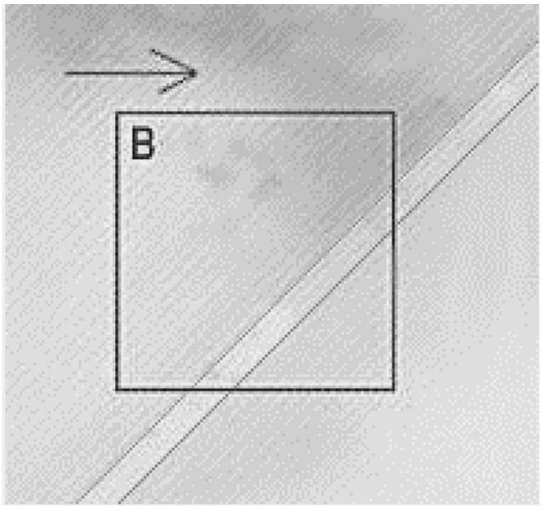

(a)

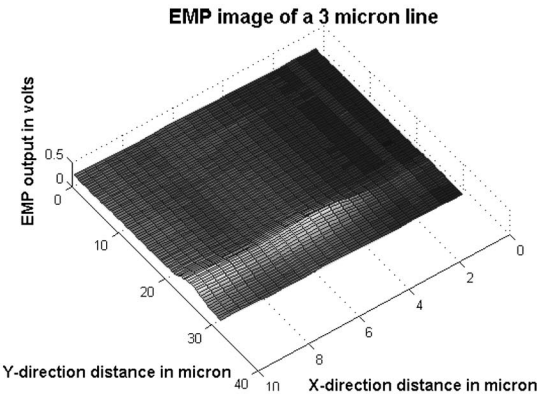

(b)

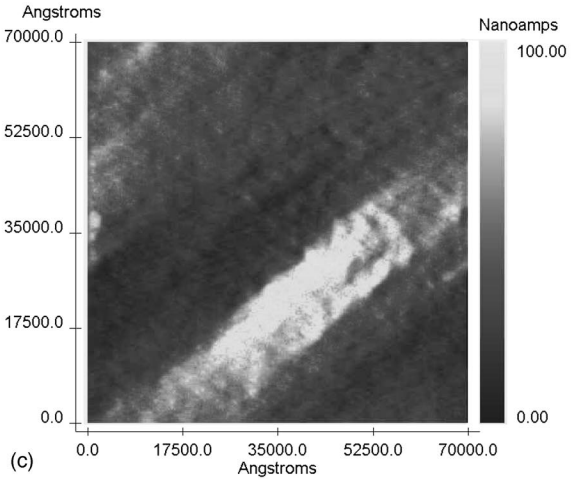

(c)

FIG. 7. (a) 3D EMP image of a 2 μm straight line (area B). (b) The optical image of the same 2 μm straight line (area B). (c) The 2D STM image of that 2 μm straight line (area B).

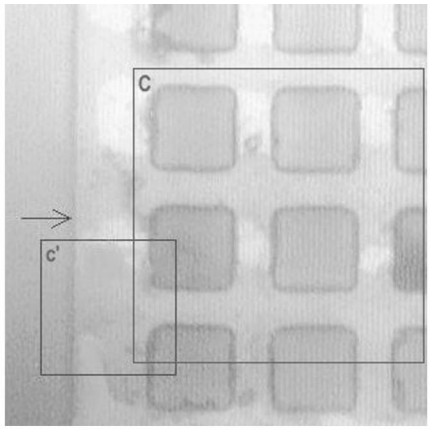

(a)

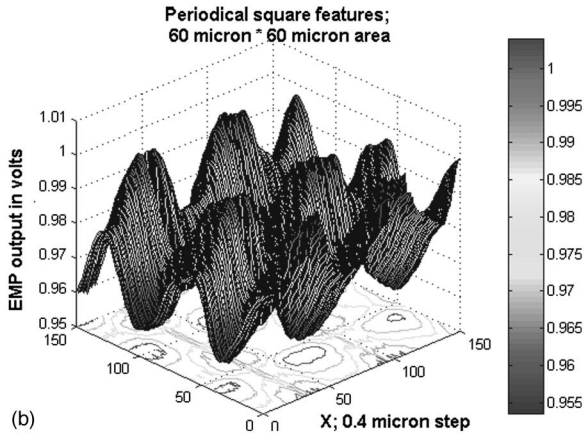

(b)

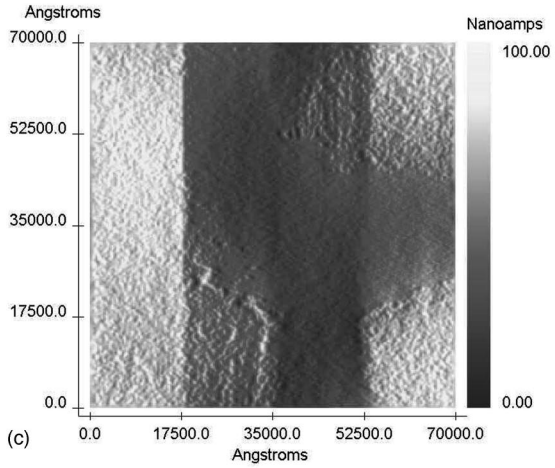

(c)

FIG. 8. (a) 3D EMP image of some 10 μm periodical square features (area C). (b) The optical image of the same 10 μm square features (area C and c′). (c) The 2D STM image shows the roundness at corners of those squares (area c′).

imaging. Figure 5 shows the area we scanned, which contains 2-μm-wide straight lines, and 10 μm periodical squares. Figure 6 is a one-dimensional (1D) EMP scan of the 2 μm straight line. It is obtained by scanning the probe over the straight line back and forth in y direction without any motion in the x direction. The full width at half maximum of the 2 μm line is 2.6 μm, while the minimum detectable signal (MDS)[5] is smaller than 0.4 μm. The 2D EMP image of the line is shown in Fig. 7(a), while the optical image and STM image of that line are also presented in Figs. 7(b) and 7(c), respectively. Finally, the EMP image, optical image, and STM image of the periodical squares are shown in Figs. 8(a), 8(b), and 8(c) for comparison. On the STM image, only the edge of the periodical area is shown, because the STM has a maximum scanning range of 7 μm$\times$7 μm. In all these scanning, the EMP was operating at 965 MHz and the tip was kept at 2 μm above the sample. The STM was operating at constant-distance mode.

IV. PROBE CALIBRATION

To perform quantitative mapping of conductivity, we calibrated the probe over a wide range of sheet resistance, from 0.24 $\Omega/\square$ to 65 k$\Omega/\square$. In our experiment, we used a Signatone four-point probe, together with Keithley 182 sensitive digital multimeter and 202 programmable current source, to measure the sheet resistance of different samples. With this highly sensitive setup, a change of 10^{-4} in surface resistance could be detected, and the deviation was below 2%. Then EMP was used to measure the microwave resistivity of these samples. For each sample, a fiber optic distance sensor was used to adjust the probe–sample distance to be exactly 2 μm to ensure the reproducibility. Silicon wafers with different doping were used as the calibrating samples, not only because of their large range of sheet resistance, but also because they had optically smooth surface and nearly identical surface reflectance from sample to sample. Figure 9(a) shows the calibration results. We may see the monotonous change of EMP output with change of sample surface resistance. The accuracy of our measurement was better than 6% for samples of low resistivity, and became worse (50% off) for high resistivity samples. This is expected since it is well known that a four-point probe is not suitable for measuring high resistivity sample.

We also used an optical method to perform fine calibra-

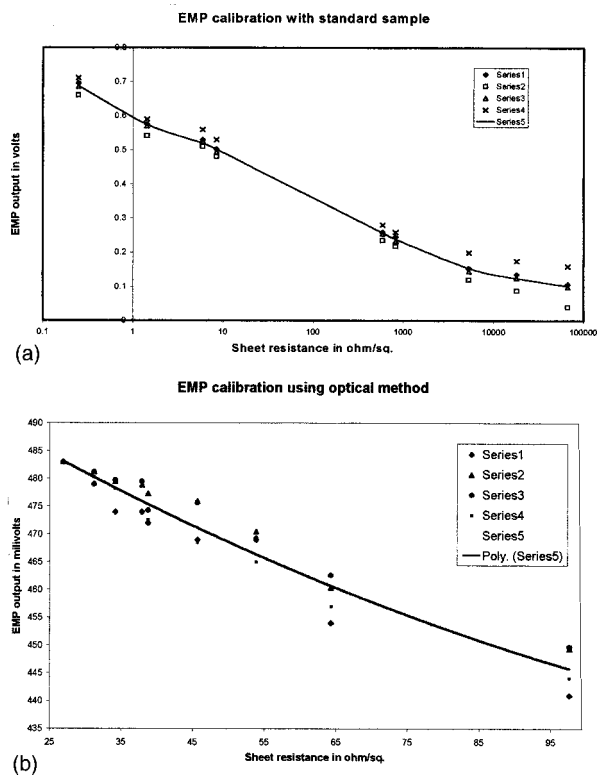

FIG. 9. (a) Evanescent microwave probe calibration using silicon samples of different resistivities. (b) Evanescent microwave probe calibration using optical method.

tion for a certain range of resistivity. One lightly doped silicon wafer was used as calibrating sample. Lights of different intensity were shone onto the wafer, each time the sheet resistance was measured using a four-point probe. Then the EMP measurement was performed with the silicon wafer illuminated with exactly the same intensities as before. Each time the EMP output was recorded to match the four-point probe output, which corresponds to a unique sample sheet resistance. The experimental result is shown in Fig. 9(b). The advantage of this technique was that there was no change for both the probe–sample distance and the surface reflectance, therefore it eliminated the dependence of EMP output on these factors. In contrast to the previous one, this calibration technique is only applicable for high resistance samples, because strong illumination will heat up the sample resulting in a change in the output.

In addition to sheet resistance mapping, we also investigated the ability of the EMP in quantitative mapping of dielectric constant of different samples. Figure 10 shows a 2D

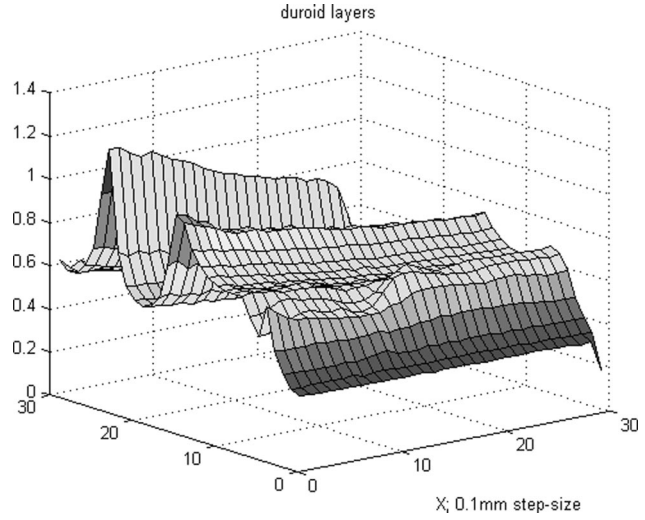

FIG. 10. 2D image of three dielectric layers of different relative dielectric constant.

map of dielectric regions next to each other, each of 1 mm wide. The first large peak is obtained for a region (Duroid) with dielectric constant of 11.8. The second peak is contributed by a region of 5.5 relative dielectric constant, while the third layer detected as the third peak is a region of 3.6 relative dielectric constant. The minimum detectable change in relative dielectric constant is calculated to be 1.7% (by MDS definition).

The detection and resolution of the EMP at 1 GHz is much better than 0.4 μm. Currently, it is limited by the minimum step size of the X-Y stage (driven by stepper motor) and the stage registration problem. To solve these problems, a piezoelectric positioning X-Y-Z stage is under construction. The piezoelectric positioner will also reduce the mechanical oscillation during scanning, and therefore improve the S/N ratio.

ACKNOWLEDGMENTS

The authors thank H. Rajgopal for preparing MEMS samples and B. Muller for developing the system software.

[1] E. A. Ash and G. Nicholls, Nature (London) **237**, 510 (1972).
[2] M. Tabib-Azar, N. Shoemaker, and S. Harris, Meas. Sci. Technol. **3**, 583 (1993).
[3] D. E. Steinhauer, C. P. Vlahcos, S. K. Dutta, F. C. Wellstood, and Steven M. Anlage, Appl. Phys. Lett. **71**, 1736 (1997).
[4] C. Gao, T. Wei, F. Duewer, Y. Lu, and X.-D. Xiang, Appl. Phys. Lett. **71**, 1872 (1997).
[5] M. Tabib-Azar, D.-P. Su, S. R. Leclair, and G. Ponchak, Rev. Sci. Instrum. (to be published).